Geophys. J. Int. (2003) **155,** 1093–1104

The interplay between global tectonic processes and the seismic cycle in the Umbria–Marche seismogenic region

Annalisa Gardi,[1,*] Roberto Sabadini,[1] Carmela Ferraro[2] and Abdelkrim Aoudia[3]

[1] *Dipartimento di Scienze della Terra, Sea. Geofisica, Università di Milano, via Cicognara 7-20129 Milano, Italy*
[2] *Telespazio SpA, CGS Space Geodesy Center, 75100 Matera, Italy*
[3] *Abdos Salam International Center for Theoretical Physics, SAND group, Dipartimento di Scienze della Terra, Univesita di Trieste, Trieste, Italy*

Accepted 2003 September 2. Received 2003 July 30; in original form 2002 June 20

SUMMARY

For the central Apennines, peninsular Italy, a series of tectonic mechanisms are reproduced by means of finite-element models, in order to study the effects of active tectonics on the seismic cycle in the Umbria–Marche seismogenic zone. Continental extension and rift push effects induced by small-scale convection are modelled within 2-D viscoelastic models of the crust–lithosphere system, in vertical cross-sections perpendicular to the strike of the major tectonic structures under study, namely the Apennines and the Colfiorito fault zone, where the 1997 seismic sequence took place. With the aim of constraining the active tectonic mechanisms at the regional scale and the behaviour of the fault in the seismogenic zone at the local scale, modelled baseline rate of change are compared with newly acquired GPS data, retrieved from the two permanent GPS receivers of Camerino (CAME) and Elba (ELBA), deliberately installed along the modelled transect. These receivers are located at both edges of the continental extension in the front of the Apennines, close to the Adriatic Plate in the east, and in the rear of the chain, in the Tyrrhenian domain. The deformation pattern inferred from seismicity and from the geodetic data is consistent with small-scale convection in the Tyrrhenian domain, which reproduces extension in the rear of the Apennines and compression in the front of the chain. A convective mechanism, associated with backarc opening and doming of the asthenosphere, provides an extensional rate, along a baseline connecting two sites in the front of the chain (Camerino) and in its rear (Elba), comparable to the observed baseline rate of change. The viscosity of the lower crust plays a fundamental role in determining the style of stress in the crust–lithosphere system. Once constrained by means of the extensional baseline rate inferred from GPS, the modelled slip across the Colfiorito fault and the modelled earthquake recurrence time are consistent with the 1997 normal fault event and with palaeoseismicity, respectively.

Key words: Apennines, central Italy, numerical modelling, seismic cycle, tectonics.

1 INTRODUCTION

The purpose of this work is to analyse the interaction between global tectonics and local scale seismicity in a selected region of the Mediterranean, the central Apennines. Several results have been published on the modelling of tectonic processes in the Apennine region and the study of their influence on crustal motions or stress and strain accumulation using different approaches (e.g. Malinverno & Ryan 1986; Bassi & Sabadini 1994; Giunchi *et al.* 1994; Faccenna *et al.* 1996; Carminati *et al.* 1999, 2001; Negredo *et al.* 1999a,b). However, none of these has focused on the relation between tectonics and the seismic cycle within a selected seismogenic zone. In this work we study the influence of global scale tectonics on the seismic cycle of the Colfiorito fault, responsible for the Umbria–Marche 1997 sequence.

The Apennines developed in a region affected by the collision between Africa and Eurasia and by the subduction of the Adriatic lithosphere. The tectonic evolution of the chain started in the Oligocene, when a collisional phase took place due to the convergence between the Sardinia–Corsica block and the Adriatic domain (Boccaletti *et al.* 1983). Extension, initially in a west–east and evolving in a northwest–southeast direction (Patacca *et al.* 1990), started in the Late Oligocene with the opening of the Algero–Provençal Basin, west of Corsica–Sardinia (Rehault *et al.* 1984), it continued with the opening of the Northern Tyrrhenian Basin in the Middle–Late Miocene (Lavecchia 1988; Sartori 1989) and migrated southeastwards with time (e.g. Spadini *et al.* 1995). This eastward migration through time of the extensional tectonics in the Tyrrhenian

*Now at: IRSN (Institut de Radioprotection et Sûreté Nucléaire), Fontenay-aux-Roses, France. E-mail: annalisa.gardi@irsn.fr

Basin and of the external compressional front is a peculiarity of the evolution of the Apennine chain (Ricci Lucchi 1986) and has been interpreted as being due to different geodynamic mechanisms. Malinverno & Ryan (1986) proposed an interpretation based on a mechanism of trench retreat or roll-back of the subducting Adriatic lithosphere that would cause the opening of a backarc basin. An alternative interpretation has been proposed (e.g. Wezel 1982), which considers the asthenospheric upwelling related to the rifting process in the Tyrrhenian Sea, as a forcing geodynamic mechanism. Furthermore, Cavinato & De Celles (1999) proposed that the bimodal state of stress in the Apennines is maintained by corner flow in the mantle wedge beneath the crest of the range. Subduction in central Italy is suggested by the presence of seismicity down to 90 km (Selvaggi & Amato 1992) and by geochemical analyses of the northern Apennine arc magmatism (Serri *et al.* 1993). However, Spakman (1990), on the basis of tomographic results and the reduced seismicity at intermediate levels, suggested that the slab may be totally or partially detached, while Amato *et al.* (1993) interpreted the presence of a high-velocity body down to 200–250 km as evidence of a continuous slab. It is thus clear that the tectonic setting of northern Apennines is very complex and that a final explanation of the role of the several ongoing processes has not been reached yet.

A finite-element technique is used to model the stress pattern along a vertical cross-section in central Italy perpendicular to the Apennines: this approach improves our understanding of the active tectonic processes in the region under study. In order to analyse the influence on the stress field from various tectonic mechanisms, several different models have been performed, each one characterized by different driving forces. We investigated the effects of the negatively buoyant subducted Adriatic lithosphere, the effects of the extensional SW–NE oriented forces expected from the counterclockwise motion of the Adriatic Plate and the effects of small-scale convection at the bottom of the Tyrrhenian lithosphere driven by the change from a passive to active rifting mode (Huismans *et al.* 2001). The stress distribution induced in the seismogenic part of the crust by each tectonic mechanism is compared with the stress pattern of the region deduced from earthquake focal mechanisms, borehole breakout analysis, *in situ* stress measurements and young geological deformation features (Frepoli & Amato 1997; Montone *et al.* 1999). These data are complemented by recent GPS baseline rates obtained from new GPS receivers installed along the transect under study.

In Fig. 1 (WSM2000, Mueller *et al.* 2000) the trace of the modelled section is indicated by the letters A-A′. Moving along this direction, from west to east, stress indicators change from extensional (red symbols) in Tuscany and in the internal sectors of the Apennine belt, to compressional (blue symbols) in the Adriatic Basin. Similar stress maps have been compiled by Rebaï *et al.* (1992) and Montone *et al.* (1999).

Stress changes, obtained by modelling the seismic cycle along a shallow low-angle normal fault, with strike perpendicular to the profile under study, have been superimposed on the stress field generated by the different tectonic processes. The same approach already used for the simulation of the Mexican subduction zone (Gardi *et al.* 2000) has been followed in the present work, although the modelling of the seismic cycle is more realistic in the present study. In fact, the locked and free alternating phases on the fault, reproducing the stick–slip process, are simulated in a different way with respect to the application carried out by Gardi *et al.* (2000). In that study the locking of the fault was obtained by imposing a zero *x*- and *y*-displacement to the nodes of the grid defining the fault, while the earthquake was simulated by imposing a fixed displacement to the same nodes in order to reproduce the dislocation. In the present analysis, locking is reproduced by impeding the relative motion of the two sides of the fault but leaving the fault free to move in the *xy*-plane. To simulate the occurrence of an earthquake, the two sides of the fault are left free to move one with respect to the other, along a frictionless interface, driven solely by the stress accumulated during the loading period of the active tectonics. The approach developed in the present study is more realistic than that in Gardi *et al.* (2000) and represents a substantial improvement with respect to previous modelling. It is worth emphasizing that this new method facilitates relating the slip obtained during a series of subsequent earthquakes to the earthquake recurrence time and active tectonics.

2 MODEL DESCRIPTION

In order to simulate the sinking of the Adriatic Plate underneath the Apennines and the seismic cycle on a shallow low-angle normal fault, the MARC package (MSC.Marc 2001) based on a finite-element technique has been used. The simulations were performed under a quasi-static approximation and the models are purely mechanical, since the coupling between the momentum and the temperature equations is not taken into account. Two models are considered, each one representing a 2-D vertical cross-section (Fig. 2) perpendicular to the strike of the Apennines and of the Umbria–Marche seismogenic zone, as shown in Fig. 1 by the trace A-A′. The 2-D domain is subdivided into quadrilateral plane-strain elements, creating an irregular mesh. The element density is increased around the discontinuities in order to ensure a good approximation of the solution. The modelled section is 400 km wide and 420 km deep. The simplified geometry of the plates and the thickness of the different layers have been defined following, for the crustal levels, the results of the seismic line CROP-03 (e.g. Pialli *et al.* 1998), and for greater depths, the results of tomographic studies (Piromallo & Morelli 1997; Chimera *et al.* 2003). Since the depth reached by the plunging lithosphere is still a matter of debate, two hypotheses have been tested: a depth of 90 km as inferred from subcrustal intraplate seismicity (Selvaggi & Amato 1992) and a depth of 150 km obtained from recent tomographic images (Chimera *et al.* 2003).

Other tectonic structures included in the models are the Val di Chiana and Val Tiberina ENE dipping, normal master faults (Boncio & Lavecchia 2000) indicated in Fig. 2 by the east-dipping fault west of Colfiorito, and a fault representing one of the structures that ruptured during the mainshocks of the Colfiorito seismic sequence of 1997 September, hereafter called the *Colfiorito fault*. The location, dip angle and depth of the two master faults are based on the results of the CROP-03 project (Pialli *et al.* 1998). The faults and the subduction plane are obtained with the dual-node technique (Goodman *et al.* 1968; Whittaker *et al.* 1992) and the motion along these contacts is characterized by a zero friction coefficient. In our simulations a linear viscoelastic Maxwell rheology has been assumed, with viscosities of 10^{24} Pa s for the upper crust, and of 5×10^{22} Pa s for the lithospheric mantle in agreement with tectonic models for similar regions (Whittaker *et al.* 1992; Giunchi *et al.* 1996a,b; Carminati *et al.* 1999) and with the estimate obtained by Houseman & Gubbins (1997); the asthenosphere has been fixed at the standard value of 10^{21} Pa s (Spada *et al.* 1992; Whittaker *et al.* 1992; Giunchi *et al.* 1996a,b) even if lower values have been recently proposed for the upper mantle of other regions (Hirth & Kohlstedt 1996; Pollitz *et al.* 2000). In central Italy the viscosity of the lower crust is largely uncertain and Riva *et al.* (2000) suggested a value ranging between 10^{18} and 10^{19} Pa s, lower than the 10^{24} Pa s of

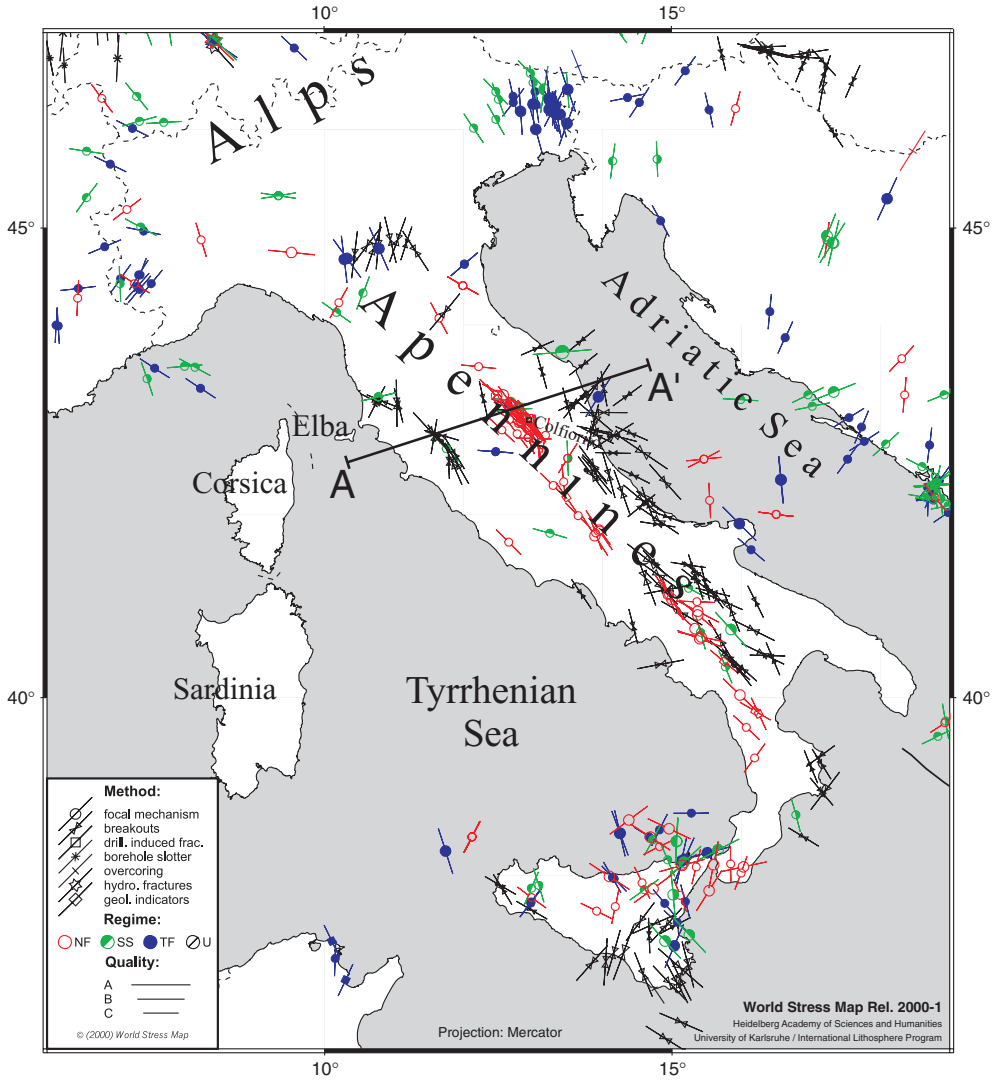

Figure 1. Stress map of Italy. Different symbols stand for different stress indicators (e.g. circles, focal mechanisms; double triangles, breakouts; squares, geological indicators). Different colours stand for different stress regime, i.e. red for extension, blue for compression, green for strike slip, while black indicates an undefined stress regime. The trace A-A′ gives the position of the cross-section modelled in this study (modified after WSM2000, Mueller *et al.* 2000).

the upper crust. As these authors also note, in order to estimate the effective viscosity of the lower crust it will be crucial to compare the results of the ongoing GPS campaigns in the Colfiorito seismogenic zone and model predictions of post-seismic deformation. All the models run with the values of 10^{24} or 10^{19} Pa s for the lower crust viscosity, which allows us to verify the sensitivity of the models to this parameter. The elastic constants are calculated following the Preliminary Reference Earth Model (Dziewonski & Anderson 1981). The model parameters for each layer are listed in Table 1.

We consider two tectonic models appropriate for continental extension (DIV) and small-scale convection following a phase of backarc opening due to subduction (CONV); these models differ only in the tectonic component, which is applied to the grid as a kinematic condition (empty arrows at the right-hand edge of the lithosphere and black arrows at the top of the asthenosphere, Fig. 2). In model DIV, a horizontal velocity of 1 mm yr^{-1} is applied to the eastern border of the grid from the surface to a depth of 70 km. This condition accounts for the extension caused by the eastward rotation of the Adria Plate. The value of 1 mm yr^{-1} has been inferred from tectonic models of the whole Mediterranean, taking self-consistency into account the counterclockwise rotation of the Adria Plate with respect to Eurasia (Jimenez Munt *et al.* 2003). The model CONV is driven by an eastward horizontal velocity where the largest value is 3 mm yr^{-1}, applied at the nodes that delineate the top of the asthenosphere in the western part of the model, namely the Tyrrhenian area (black arrows at the top of the asthenosphere, in the left portion of the model, Fig. 2). This kinematic condition does not have vertical component and it is introduced to simulate the effects of the rift push forces induced by the small-scale convection cell, which develops when the lithosphere–mantle system changes from passive to active rifting mode, due to asthenospheric doming; this modelling reproduces the coeval occurrence of extension above the convecting region and compression at its flank (Huismans *et al.* 2001). The velocity boundary condition in

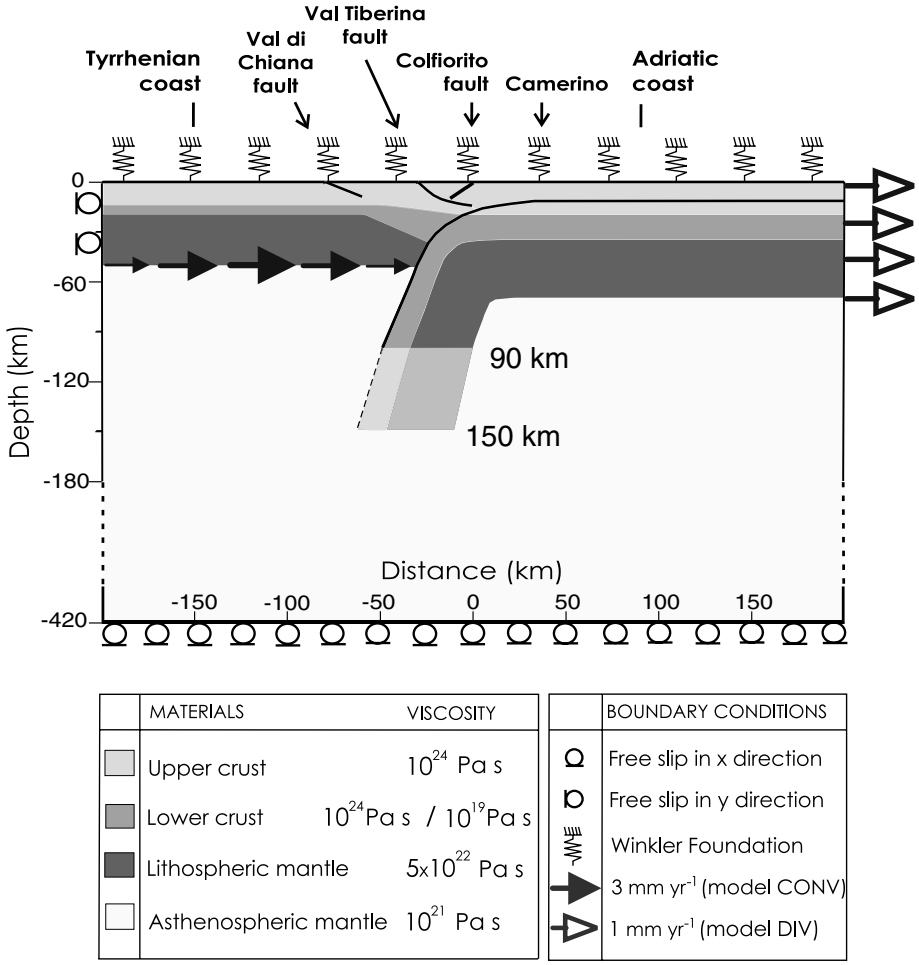

Figure 2. Geometry, materials and boundary conditions of the 2-D models. Circles indicate free-slip conditions. Spring symbols represent the buoyant restoring force applied at the upper surface. The white arrows denote the velocity applied at the top right-hand side of the model DIV, while the black arrows denote the driving velocity of the model CONV, which is applied at the top of asthenosphere in the Tyrrhenian domain. Bold continuous lines represent the contact planes.

Table 1. Mechanical properties of the materials.

	Viscosity η (Pa s)	Poisson's ratio ν	Young's modulus E (Pa)
Upper crust	10^{24}	0.27	1.75×10^{11}
Lower crust	10^{24} or 10^{19}	0.27	1.75×10^{11}
Lithospheric mantle	5×10^{22}	0.27	1.75×10^{11}
Asthenospheric mantle	10^{21}	0.27	1.75×10^{11}

the CONV model has a sinusoidal shape (Fig. 2), in agreement with the pattern of the velocity field in convective problems (Turcotte & Shubert 2001) and induces a deformation pattern similar to that induced by the DIV model in the region around the Colfiorito fault, which makes the CONV and the DIV models comparable in terms of the absolute velocity of the seismogenic zone with respect to the left-hand edge of the models.

Other mechanical boundary conditions are applied as follows. The bottom border of the grid has been fixed in the vertical direction while the western border corresponding to the lithospheric level is fixed in the horizontal direction to account for the presence of the strong lithosphere of the Corsica–Sardinia block. No boundary conditions are applied to the remaining vertical boundaries. This implicitly means that these boundaries are left free, this allows for the horizontal flow of the material. Gravity is applied to all the elements of the meshes, not as a body force, but as an additional boundary condition, with a value of 9.8 m s^{-2}. The isostatic restoring forces are easily taken into account using the method known as the *Winkler foundation* (Desai 1979). This technique consists of applying, at the boundary between different materials, a vertical pressure proportional to the changes in density and to the computed vertical displacement. For simplicity this force (spring symbols in Fig. 2) is applied only where the density contrast is the greatest, that is at the upper free surface of the models, which is the boundary between the crust and the atmosphere, neglecting the internal density contrasts between the crust and the upper mantle.

The simulation of the tectonic loading and of the seismic cycle is subdivided into several steps (Table 2). The first step has a duration of 250 kyr; this time interval is necessary for the model to reach a dynamic equilibrium between the tectonic and isostatic forces and for stress and strain rates to reach steady-state values (Giunchi *et al.* 1994, 1996b). Once the steady state is attained, it is possible to model the seismic cycles. The second step of these simulations has a duration of 100 yr corresponding to the phase of loading during the cycle, or the interseismic period. During this time step the Colfiorito fault is locked and stress accumulates in the region surrounding the seismogenic zone. The locked condition is realized by impeding slip on the main fault zone. The third step has a nominal duration

Table 2. Simulation strategy.

Step	Contact condition at the Colf. fault	Step duration
First	Free	250 kyr
Second	Locked	100 yr
Third	Free	60 s
Fourth	Locked	100 yr
Fifth	Free	60 s
Sixth	Locked	100 yr
Seventh	Free	60 s
Eighth	Locked	100 yr
Ninth	Free	60 s
Tenth	Locked	100 yr
11th	Free	60 s
12th	Locked	100 yr

of 60 s, which is meant to simulate the instantaneous occurrence of the earthquake: the fault is left free, slip occurs on the fault plane and the stress is released. A new cycle then begins; during the fourth step the fault is locked again for 100 yr, during the fifth step a second earthquake is simulated and so on, up to five earthquakes.

3 MODELLING RESULTS

The results of the simulations are presented in Figs 3–6 and 8–9 (see below). Figs 3–6 consist of two panels: the stress eigenvalues and eigenvectors, red denoting extension and blue denoting compression, are shown in the top panels while the velocity field is shown in the bottom ones. Both the stress and velocity fields are shown at time $t = 250.1$ kyr after the beginning of the simulation, i.e. at the end of the second step in Table 2, when steady-state stress values have been reached in the crust–lithosphere system. The origin of the horizontal axis is chosen in such a way as to coincide with the point in which the Colfiorito fault, a line in the vertical cross-section, pierces the model surface. We also show the results of some tests in which the Val di Chiana and Val Tiberina master faults have been activated in order to study their influence on the stress pattern. Fig. 8 (see below) shows the modelled baseline rate between the two GPS sites of Camerino (CAME) and Elba (ELBA), while Fig. 9 (see below) shows the slip across the Colfiorito fault for the different models.

Before presenting the results of DIV and CONV models, it is worth mentioning that we also tested the slab pull mechanism as the only driving mechanism of the model. In order to simulate the slab pull effects, a positive density contrast of 80 kg m^{-3} is assigned to the deepest portion of the subducting crust. This density anomaly, resulting from the phase transformation of a subducting plate when it exceeds a depth of approximately 90 km, is based on the petrological studies of Irifune & Ringwood (1987). The depth of the subducting plate used in these simulations is of 150 km, as shown in Fig. 2. At first, the lower crust viscosity is fixed at 10^{24} Pa s. The results are in distinct contrast with the observed style of faulting in the Colfiorito seismogenic zone, where normal faulting is the dominant mechanism instead of the thrust one obtained with this test. Predicted stress values are low, at most 10 MPa in the subducted plate. Selecting a lower crust viscosity of 10^{19} Pa s and maintaining slab pull as the driving force, the stress intensity is substantially reduced, due to the reduction in the stiffness of the lower crust, and the stress pattern is dominated by extension, except in a region of the upper crust embedded between the Val Tiberina and the Colfiorito fault, where compression is still the dominant style of stress. These results are not satisfactory, because the Colfiorito seismogenic zone is subject to compression, in disagreement with seismic data.

On the basis of these simulations, slab pull does not seem to be a feasible mechanism in the central sector of the Italian peninsula, in agreement with Negredo *et al.* (1999b), mainly because of the compressional state of stress obtained around the Colfiorito seismogenic zone. However, recent shallow tomographic studies (e.g. Chimera *et al.* 2003) have shown that the Colfiorito fault displays a typical thrust fault geometry as also supported by seismic reflection and geological data (Bally *et al.* 1986; Meghraoui *et al.* 1999). This would favour the slab pull mechanism as a prevailing process acting on the Colfiorito fault before its inversion to the present-day normal-faulting mechanism.

Fig. 3 shows the results obtained for model DIV considering a lower crust viscosity of 10^{24} Pa s. The most notable feature of the stress pattern is the predominant extension affecting the whole upper crust, while the lower crust undergoes compression. The orientation of the extensional stress axes in the upper and lower crust reveals how these layers respond to the applied loads and boundary conditions. The upwarping of the knee of the subducted plate causes an upward bending of the upper crust between the Chiana and Tiberina valleys and induces compression in the lower crust. In response to this upwarping the crust downbends around the Colfiorito area, generating some compression near the shallower edge of the Colfiorito fault. This model can thus retrieve the extensional tectonic style observed in Tuscany and in the inner portion of the Apennines, but not the compression observed in the external part of the belt, towards the Adriatic Basin. Fig. 3(b) depicts the velocity field, which is mostly horizontal and eastward oriented, in agreement with the direction of the velocity applied as a driving mechanism for this model. Velocity values of the order of 1–1.5 mm yr^{-1} are comparable to the kinematic boundary conditions applied at the right-hand edge of the model. A marked downward velocity zone around Colfiorito is consistent with the downbending inferred from the stress style in proximity of this seismogenic zone.

We have verified that since the slab pull is not active and thus there is no density contrast at depth during simulations, the maximum depth reached by the slab (90 or 150 km) does not affect the stress and velocity fields.

In the remaining models, the lower crust viscosity is fixed at 10^{19} Pa s, in agreement with the value of the ductile lowermost part of the crust indicated by the results of post-seismic deformation studies in the area (Riva *et al.* 2000) and with the work by Cosgrove (1997), who shows that a lower crust, which is undergoing extension, experiences bulk rheological changes during deformation, which reduces its viscosity.

The stress field computed by means of model DIV, characterized by a lower crust viscosity of 10^{19} Pa s is portrayed in Fig. 4(a), with some remarkable differences with respect to Fig. 3(a). The most notable difference with respect to Fig. 3(a) is the almost total absence of compression in the lower crust. In response to the lowering of the viscosity from 10^{24} to 10^{19} Pa s, the stress style in the lower crust changes from compression (Fig. 3a) into extension (Fig. 4a). In general, the stress intensity is reduced in the whole model with respect to Fig. 3(a). A smooth velocity pattern is obtained in the contact region between the knee of the subducted plate and the lower crust, which implies the absence of bending. Furthermore, with respect to Fig. 3(a), compression disappears in the vicinity of Colfiorito. The smooth velocity field agrees well with the lower stress intensity values attained in the crust–lithosphere system. The velocity field is essentially horizontal, eastward oriented and, in general, more

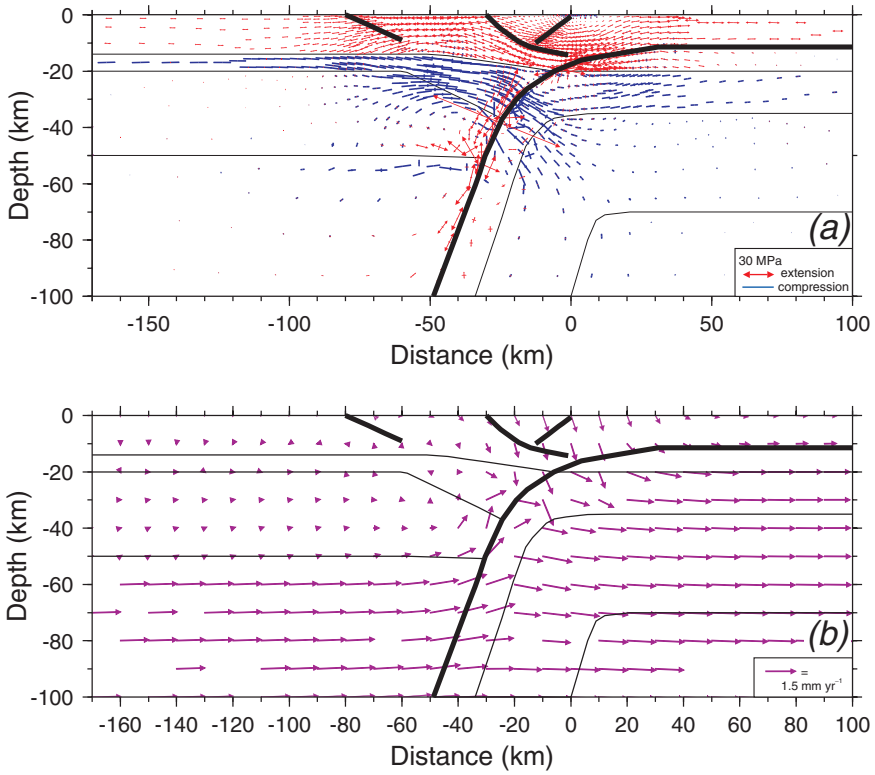

Figure 3. Results obtained with model DIV, with a lower crust viscosity of 10^{24} Pa s and a driving velocity of 1 mm yr^{-1}. (a) Major eigenvectors for the stress tensors, red indicates tension and blue compression. (b) Velocity field in mm yr^{-1}.

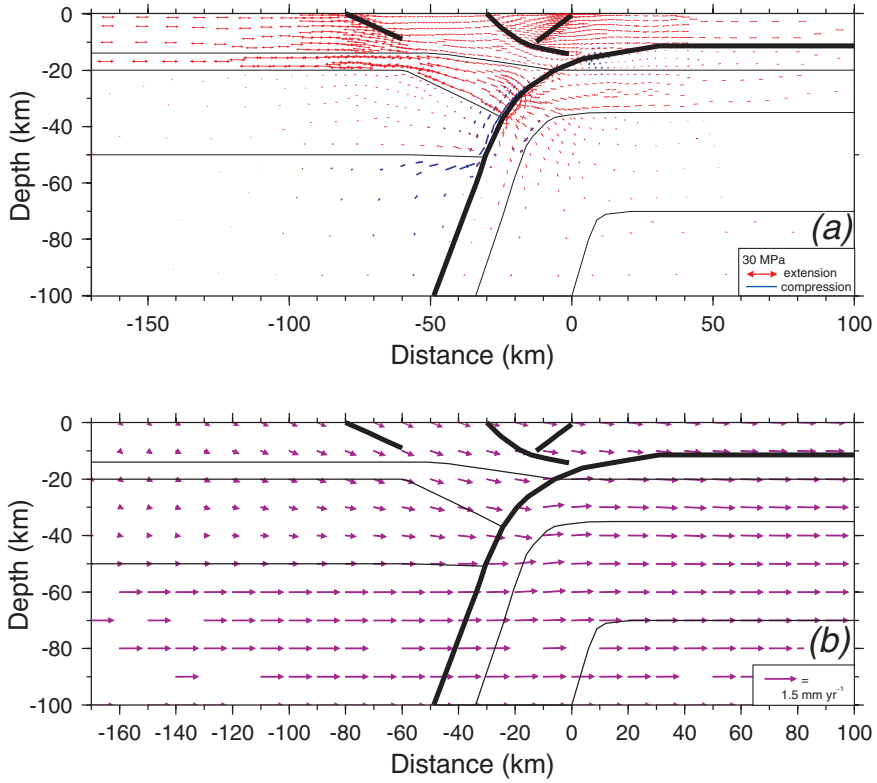

Figure 4. Results obtained with model DIV, with a lower crust viscosity of 10^{19} Pa s and a driving velocity of 1 mm yr^{-1}. Same representation as in Fig. 3.

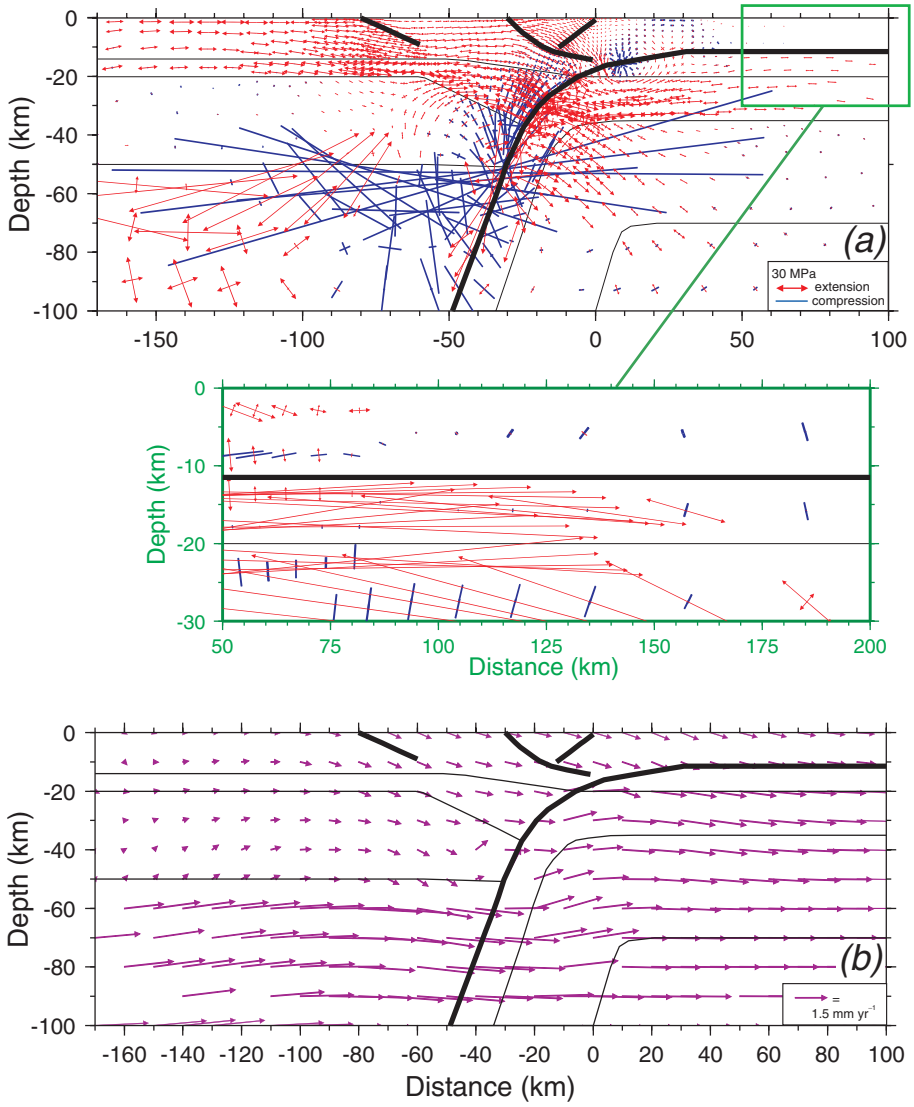

Figure 5. Results obtained with model CONV, with a lower crust viscosity of 10^{19} Pa s and a driving velocity of 3 mm yr^{-1}. Same representation as in Fig. 3.

regular than that characterizing the previous DIV model with a hard lower crust (Fig. 3b). These phenomena are related to the decoupling between the upper crust and the lithospheric mantle, due to the stress relaxation occurring in the lower crust. The whole upper crust undergoes extension and the model fails to reproduce compression in the outer margin of the Apennines.

Fig. 5 depicts the stress and velocity fields produced by the CONV model, characterized by a lower crust viscosity of 10^{19} Pa s. Extension accumulates in the whole lower crust, in the upper crust in Tuscany and in the Colfiorito seismogenic zone. As a result of the reduced intensity of stress within the crust, the stress axes near the Adriatic coast are not visible at the same scale as that used in the previous figures. The enlargement of the portion of the crust embedded in the green rectangle shows that some amount of compression accumulates in the transition zone between the Apennines and the Adriatic domain, even though it is of low intensity.

The kinematic condition applied at the nodes of the top portion of the mantle, as shown in Fig. 2, is responsible for the appearance of compression in the wedge overlying the subducted portion of the plate, which could be in agreement with the upwelling of asthenospheric material, as heat flow data suggest (Mongelli *et al.* 1991; Mele *et al.* 1997; Piromallo & Morelli 1997). The CONV model can thus reproduce the extension observed in Tuscany and in the internal sectors of the Apennines, including the Colfiorito seismogenic zone, and the compression in the external part of the chain and Adriatic domain. The intensity of the extensional stresses in the crust is comparable to the results of the previous figures, although obtained from a different tectonic mechanism. The velocity field, Fig. 5(b), resembles that induced by the DIV model. The velocity in the lithosphere portrays a dominant eastward component and a pattern within the sinking lithosphere, which is also typical of a slab-retreat motion, in agreement with the mechanism proposed by Malinverno & Ryan (1986).

Finally, a simulation based on CONV and on the activation of the Val di Chiana and Val Tiberina master faults, shows the stress and velocity fields depicted in Fig. 6. Comparison with Fig. 5(a) shows that the presence of two crustal structures undergoing a free slip condition significantly changes the stress field in the region around the structures themselves. From west to east, the footwall block of the Chiana fault undergoes a rotation of the tensional axes towards a direction perpendicular to the fault. Between the two master faults, the stress intensity drops significantly and the stress axes rotate in

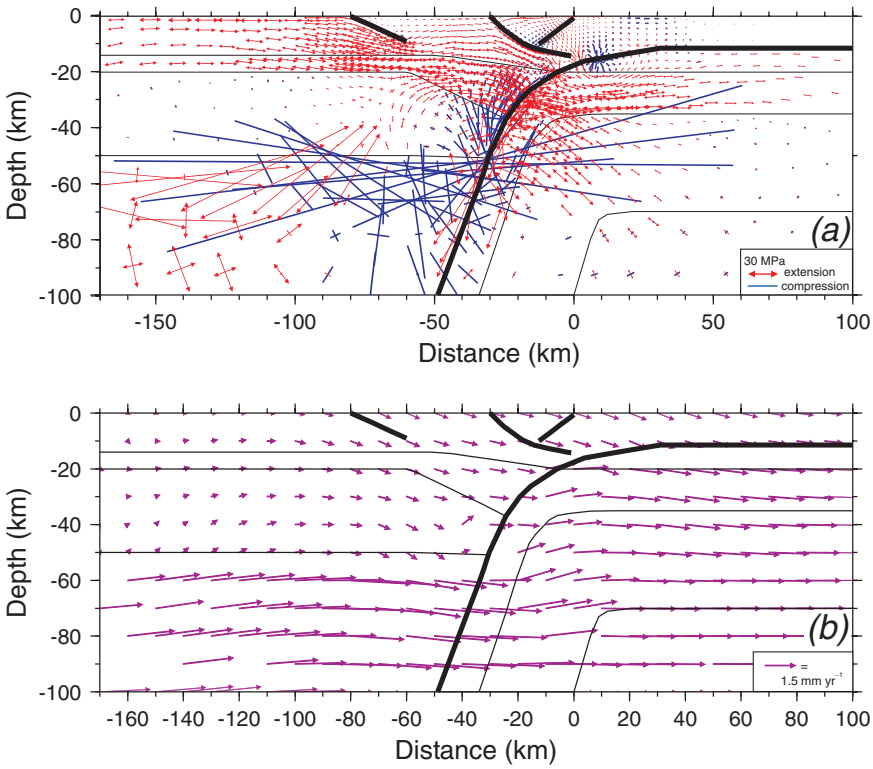

Figure 6. Results obtained with model CONV when the Val di Chiana and Val Tiberina master faults are activated, with a lower crust viscosity of 10^{19} Pa s and a driving velocity of 3 mm yr^{-1}. Same representation as in Fig. 3.

proximity of the Tiberina fault, as found for the Val di Chiana fault. Compressional stresses accumulate around the downdip edge of the Colfiorito fault, causing the inversion of its faulting mechanism from normal to thrust. The stress pattern shown in Fig. 6 represents the situation at the end of the second step of the simulation (Table 2), that is just before the first earthquake. In the following step, when the Colfiorito fault is left free, due to the stress pattern shown in Fig. 6(a), a thrust faulting mechanism is produced. This mechanism disagrees with the normal-faulting mechanism deduced for the earthquake sequence of 1997 September in central Italy (Amato *et al.* 1998). The velocity field (panel b) is not affected by the activation of the two master normal faults, which indicates that the interplay between the three faults does not modify the global velocity pattern induced by the tectonic mechanism.

Among the various models, CONV based on 10^{19} Pa s for the lower crust is the most appropriate for reproducing extension in Tuscany and in the inner portions of the Apennine belt, compression near the Adriatic margin and normal-faulting in the Colfiorito seismogenic zone.

Fig. 7 shows the baseline rates inferred from two new permanent GPS receivers installed along the transect modelled in the present analysis, in Camerino (CAME), 20 km east of Colfiorito, and in the Elba island (ELBA), in the Tyrrhenian coast of Italy. Three baselines are portrayed, CAME–CAGL, CAME–ELBA and ELBA–CAGL, with Cagliari (CAGL) located in the island of Sardinia. These permanent sites monitor the deformation between Camerino and Elba, responsible for the extension and for the normal fault seismicity in the Colfiorito seismogenic zone and for the deformation style of the northern Apennines. These baselines include the estimated velocity of the CAME site, which is based on a coordinate time-series of two years, resulting in a reliable GPS velocity; the ELBA site has a

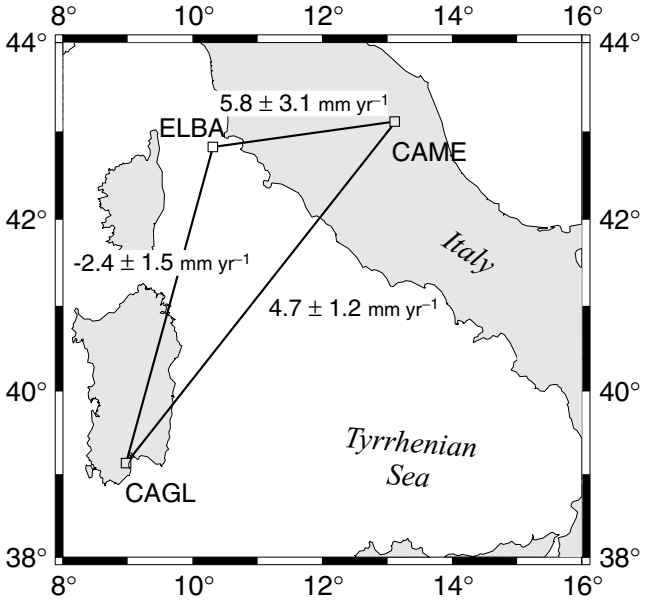

Figure 7. Baseline rates, in mm yr^{-1}, inferred from permanent GPS receivers installed in Camerino (CAME) and Elba island (ELBA).

shorter history (coordinate time-series covering one year), implying that the velocity of this site may be subject to variations.

Baseline rates are computed from the ASImed GPS-VLBI-SLR combined solution (GEODAF, 2002, geodaf@mt.asi.it). The three geodetic techniques are co-located at the Cagliari site, but also affect the solutions at CAME and ELBA, due to cross correlation. Both CAME–CAGL and CAME–ELBA indicate extension between the

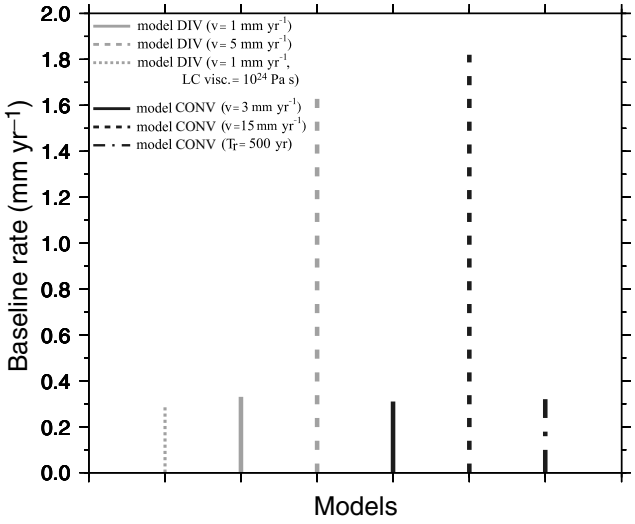

Figure 8. Modelled baseline rates between Camerino and a point located in Tuscany, 120 km west from Colfiorito, representative of the Elba site. Grey lines represent the results obtained with model DIV driven by a velocity of 1 mm yr^{-1} when lower crust viscosity is 10^{24} Pa s (dotted) or 10^{19} Pa s (solid), and model DIV driven by a velocity of 5 mm yr^{-1} with a lower crust viscosity of 10^{19} Pa s (dashed). Black lines give the results of model CONV with 10^{19} Pa s as lower crust viscosity and driving velocities of 3 mm yr^{-1} (solid), 15 mm yr^{-1} (dashed), and again 3 mm yr^{-1} with an interseismic period increased to 500 yr (dash-dotted).

portion of the Apennines where the Camerino site is located and the Tyrrhenian domain, at a rate of 4.7 ± 1.2 and 5.8 ± 3.1 mm yr^{-1}, respectively. Although the two baselines are not parallel, they both indicate extension, mainly occurring within the Italian peninsula rather than in the Tyrrhenian Basin, as suggested by the two comparable rates. The ELBA–CAGL baseline indicates shortening at a rate of -2.4 ± 1.5 mm yr^{-1}, which could be ascribed to the global Africa–Eurasia convergence. These GPS baselines show for the first time the motion of the northern Apennines with respect to the Tyrrhenian domain and the extension in the rear of the chain, which agrees well with the extensional seismicity occurring in this region.

Fig. 8 shows the modelled baseline rates of the Camerino site (CAME) relative to a point located −120 km west of Colfiorito, representative of the Elba site, in the Tyrrhenian coast (see also Fig. 2). For both models DIV and CONV, grey and black lines, the baseline rate is obtained in the steady state by evaluating the variation in the distance between the two sites in one year, at the end of the earthquake cycles simulation (step 12 in Table 2). These two models are driven by a velocity of 1 mm yr^{-1} at the right-hand edge of the lithosphere (DIV, grey, continuous line) and by a velocity of 3 mm yr^{-1} (CONV, black, continuous line) at the top of the Tyrrhenian asthenosphere, which guarantees that the deformation at the surface in the seismogenic zone is comparable for the two models. Two cases are also shown, in which the driving velocities are increased by a factor of 5 (dashed, grey and black). Moreover, a case is considered in which the interseismic period is increased to 500 yr (CONV, black, dash-dotted) and one in which the viscosity of the lower crust is fixed at 10^{24} Pa s (DIV, grey, dotted). In all the other cases, the interseismic period is 100 yr, as in Table 2, and the viscosity of the crust is 10^{19} Pa s, in agreement with the considerations given in the description of the previous figures.

Comparison between the continuous lines, grey and black, shows that the baseline rate is comparable for the two models DIV and CONV, ∼0.3 mm yr^{-1}, respectively, as expected, since the driving velocities have been deliberately chosen in order to make the two models comparable as far as the deformation within the seismogenic zone is concerned. Both models are subject to a linear increase of approximately a factor five in the baseline rate, when the driving velocities are increased to 5 and 15 mm yr^{-1}, respectively, in DIV and CONV (dashed lines, grey and black). The DIV model increases from 0.3 to 1.6 mm yr^{-1}, while CONV increases from 0.3 to 1.8 mm yr^{-1}. The model portraying the lowest baseline rate of 0.25 mm yr^{-1} is that characterized by the stiff lower crust, namely model DIV with lower crust viscosity of 10^{24} Pa s, dotted grey. Comparison between the dotted and continuous light grey lines, shows that the stiffening of the lower crust has a minor effect in reducing the baseline rate, once a steady state has been attained by the model.

Within the model CONV, the recurrence time is varied within the seismic cycle, increasing this parameter to 500 yr, maintaining the driving velocity at 3 mm yr^{-1}: the results are provided by the black dash-dotted lines. The minor modifications with respect to the continuous lines, indicates that, at steady state after the seismic cycles, the baseline rates due to the global tectonic processes is unaffected by the recurrence time of the earthquakes. These modelled baseline rates can be compared with the CAME–ELBA and CAME–CAGL baseline rates. The largest driving velocities for the two DIV and CONV, 5 and 15 mm yr^{-1}, respectively, induce a baseline CAME–ELBA extensional rate of 1.6–1.9 mm yr^{-1}, respectively, grey and black dashed, comparable to the lower limit of 2.7 mm yr^{-1} of the observed CAME–ELBA baseline rate. The baseline rates obtained by making use of the lowest driving velocities are inconsistent with the observed values, independent of the viscosity of the lower crust (grey dotted) or the earthquake recurrence time (dash-dotted). Although this comparison must be taken with caution due to the still short period of acquisition time, especially for the ELBA site, the model results and the geodetic solutions indicate that the tectonic mechanisms considered in our analysis are consistent with the newly acquired GPS data, even though other tectonic mechanisms cannot be ruled out. It is worthwhile emphasizing, that the vertical deformation rates of the CAME site, not shown in our study, include motion, which is comparable to the noise. The CAME site is thus affected mainly by horizontal motions, which seems to exclude tectonic mechanisms that involve important vertical deformation, such as the slab detachment mechanism (Wortel & Spakman 2000) or any other one associated with important isostatic disequilibrium of the Apennines.

Fig. 9 shows the slip obtained during the seismic cycle, for the DIV and CONV models, for the same parameters and symbols of Fig. 8, except for the extra simulation portrayed by the dash-dotted-dotted curve, relative to a recurrence time of 500 yr and a driving velocity of 15 mm yr^{-1} in CONV. The earthquake number within the cycles is given on the horizontal axis, while the slip across the fault surface is given on the vertical axis.

The slip values range between several metres during the first earthquake to centimetres at steady state. The large amount of slip during the first earthquake is not realistic, since it is obtained for faulting occurring after a long period of 250 kyr of continuous tectonic loading. Thus we can only compare the slip of the real earthquake with the modelled slip at steady state, which is attained after the second or third earthquake depending on the model. Both DIV and CONV, driven by the lowermost tectonic velocity of 1 and 3 mm yr^{-1} predict a 2 cm slip at most, this value attained by the DIV model for the stiff

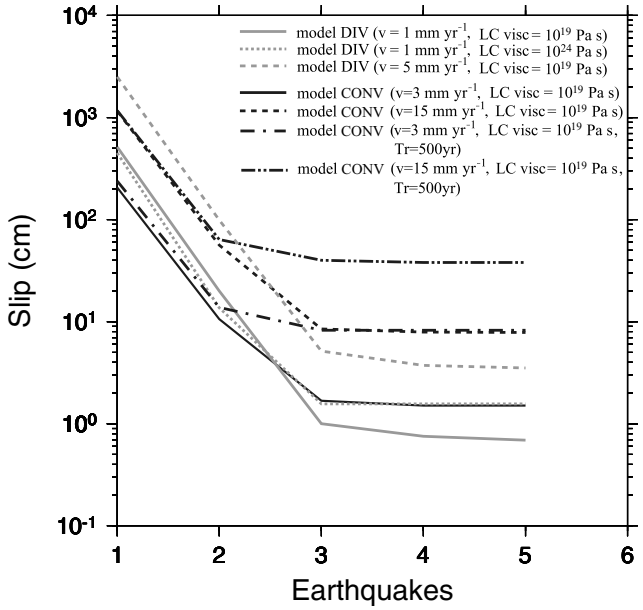

Figure 9. Slip obtained during the simulated seismic cycles for the different models. Same representation as in Fig. 8, except for the additional dash-dotted-dotted curve for an extra computation performed with a 500 yr recurrence time and a driving velocity of 15 mm yr^{-1} in the CONV model.

lower crust of 10^{24} Pa s (grey dotted and black continuous). If the lower crust is 10^{19} Pa s, the slip of the DIV model is negligible (grey continuous). The increase in the driving velocity to 5 and 15 mm yr^{-1}, is responsible for an increase up to 4 and 9 cm for the slip corresponding to the DIV and CONV models, grey and black dashed curves. These values are lower than the 66 cm of slip estimated by Hunstad *et al.* (1998) for the 1997 Colfiorito earthquake. In analogy with the calculations of the previous figure, the recurrence time T_r has been increased to 500 yr, black dash-dotted curve, maintaining the driving velocity constant at 3 mm yr^{-1}, as in the case depicted by the black continuous curve. Although a substantial increase up to 9 cm is obtained for the slip, as for the case of 100 yr recurrence time and driving velocity of 15 mm yr^{-1}, the slip is still substantially lower than that estimated for the real earthquake.

The steady-state values of the CONV models, black dashed and dash-dotted curves, clearly show that a trade off exists between the driving velocity and the recurrence time of the earthquake and also show that increasing the driving velocity or the recurrence time independently from one another, does not increase the slip on the fault. For that reason, another test has been performed increasing both the driving velocity and the recurrence time. The result is shown by the black dash-dotted-dotted curve, where from the second to the fifth earthquake a slip of 64 and 40 cm is obtained, with a steady-state value that is now comparable to the observed one. It is clear that an increase in the recurrence time would allow a closer fit with the estimated value of 66 cm, but it is not the aim of the present analysis to carry out a parameter variation study, in order to reproduce the slip across the Colfiorito fault.

Palaeoseismicity provides with a recurrence time for the September 26 Colfiorito earthquake ranging between 700 and 3700 yr (Valensise & Pantosti 2001). The lower limit of 700 yr agrees with the 500 yr modelled recurrence time that let us obtain an order of magnitude of the slip across the fault (Fig. 9) comparable to the slip inferred from seismological data. The fact that the recurrence time of 500 yr is not the only ingredient that is necessary to fit the slip, but must be accompanied by a modelled baseline rate between Camerino and sites in the Tyrrhenian domain, which agrees well with the new CAME data, is a strong indication, although not definitive proof, that all the major phenomena that impact the seismic cycle in the studied portion of the Apennines have been taken into account properly. It is worth mentioning that our results on the slip on the fault should be taken with caution, due to our approximation of treating a 3-D structure such as the Colfiorito fault by means of a 2-D model.

4 CONCLUSIONS

The present study develops a new approach for modelling the seismic behaviour of normal faults in central Italy, relating their activity to tectonics. As the tectonic setting of central Italy is very complex and still far from being completely understood, different scenarios have been tested, including, as driving mechanisms for our models, continental extension caused by the counter-clockwise rotation of the Adria Plate and small-scale convection due to asthenospheric upwelling in the Tyrrhenian domain. Slab pull has been rejected, since it causes a vertical suction on the surface layers above the knee of the sinking plate, thus generating compressional stresses in the proximity of the Colfiorito area and inverting the fault mechanism on this fault from normal to thrust, as inferred from the earthquake sequence of 1997 September. However, it is necessary to note that the slab pull mechanism could be appropriate to reproduce the Colfiorito fault behaviour in the geological past.

A divergence applied at the easternmost boundary of the models, in order to simulate the counter-clockwise rotation of the subduction front, can be excluded as well: this mechanism reproduces the extension in the Tyrrhenian Basin and in the Apennines but fails in retrieving the compression in the Adriatic domain, in disagreement with the tectonic style observed in this region. The mechanism of active rifting, proposed by Huismans *et al.* (2001), is the most appropriate, since it retrieves extension in Tuscany and in the Apennines and some compression in the Adriatic Basin. The convection model CONV for active rifting works correctly when a lower crust viscosity of 10^{19} Pa s is considered. Otherwise, with an almost elastic lower crust, the concentration of stress within the entire lithosphere would be too high, due to the bending of the upper crust, which favours the accumulation of compressional stresses in Tuscany and Apennines, where, in contrast, an extensional regime is expected.

The second part of the work presented in this paper is the modelling of the seismic cycle. For the first time, the local scale seismicity is related to global tectonics. The package MARC is used to simulate the seismic cycle on the same fault in a realistic fashion, without imposing a fixed slip on the fault (as in Gardi *et al.* 2000), but leaving it free to slip depending on the amount of stress accumulated during the interseismic period due to the active global tectonics. This approach allows us to investigate the interplay between the slip on the fault, the deformation rate in the region and the recurrence time of earthquakes on the same fault.

The results are compared with the first available GPS data in the northern Apennines, central Italy. The convection model provides baseline rates comparable to the observed ones. This study provides the link between GPS observations, with the characteristics of the seismicity in a seismogenic zone crossed by the GPS baselines, and by the modelled sections. By modelling five subsequent earthquakes on the Colfiorito fault, a slip across the fault, comparable to the slip estimated by Hunstad *et al.* (1998) for the 1997 Colfiorito earthquake, is obtained, once the modelled baseline rates are consistent

with GPS observations. The recurrence time of the earthquakes is of the order of 500 yr, consistent with palaeoseismicity.

These results highlight the fact that the evolution of a local scale structure is influenced by mechanisms acting at the long-wavelength spatial scale characterizing the tectonic processes. This result supports the concept that seismicity is controlled by global active tectonics, although local effects due to small-scale structural anomalies at the scale of the seismogenic zone cannot be ruled out, as these have not been included in the modelling.

ACKNOWLEDGMENTS

We are indebted to Cecilia Sciarretta, Telespazio SpA and Franco Vespe, Agenzia Spaziale Italiana, Centro di Geodesia Spaziale 'G. Colombo', Matera, for their continual encouragement and support in the development of this study. This work is partially supported by the Ministry of Instruction, University and Research of Italy, through the COFIN2002 project 'A multidisciplinary monitoring and multiscale study of the active deformation in the northern sector of the Adria Plate'. We thank the two anonymous referees for their constructive remarks.

REFERENCES

Amato, A., Alessandrini, B., Cimini, G., Frepoli, A. & Selvaggi, G., 1993. Active and remnant subducted slabs beneath Italy: evidence from seismic tomography and seismicity, *Ann. Geofis.,* **36,** 201–214.

Amato, A. *et al.*, 1998. The 1997 Umbria–Marche, Italy, earthquake sequence: a first look at the main shocks and aftershocks, *Geophys. Res. Lett.,* **25,** 2861–2864.

Bally, A.V., Burbi, L., Cooper, C. & Ghelardoni, R., 1986. Balanced sections and seismic reflection profiles across the Central Apennines, *Mem. Soc. Geol. It.,* **35,** 257–310.

Bassi, G., Sabadini, R. & Rebaï, S., 1997. Modern tectonic regime in the Tyrrhenian area: observations and models, *Geophys. J. Int.,* **129,** 330–346.

Boccaletti, M., Calamita, F., Centamore, E., Deiana, G. & Dramis, F., 1983. The Umbria–Marche Apennines: an example of thrust and wrenching tectonics in a model of ensialic Neogenic–Quaternary deformation, *Boll. Soc. Geol. It.,* **102,** 581–592.

Boncio, P. & Lavecchia, G., 2000. A geological model for the Colfiorito earthquakes (September–October 1997, Central Italy), *J. Seism.,* **4,** 345–356.

Carminati, E., Giunchi, C., Argnani, A., Sabadini, R. & Fernandez, M., 1999. Plio-Quaternary vertical motion of the Northern Appennines: insights from dynamic modelling, *Tectonics,* **18,** 703–718.

Carminati, E., Toniolo Augier, F. & Barba, S., 2001. Dynamic modelling of stress accumulation in central Italy: role of structural heterogeneities and rheologies, *Geophys. J. Int.,* **144,** 373–390.

Cavinato, G.P. & De Celles, P.G., 1999. Extensional basins in the tectonically bimodal central Apennines fold-thrust belt, Italy: response to corner flow above a subducting slab in a retrograde motion, *Geology,* **27,** 955–958.

Chimera, G., Aoudia, A., Saraò, A. & Panza, G.F., 2003. Active tectonics in Central Italy: constraints from surface wave tomography and source moment tensor inversion, *Phys. Earth planet. Inter.,* **138,** 241–262.

Cosgrove, J.W., 1997. The influence of mechanical anisotropy on the behaviour of the lower crust, *Tectonophysics,* **280,** 1–14.

Desai, C.S., 1979. *Elementary Finite Element Method,* p. 434, Prentice-Hall, Englewood Cliffs.

Dziewonski, A.M. & Anderson, D.L., 1981. Preliminary Reference Earth Model, *Phys. Earth planet. Inter.,* **25,** 297–356.

Faccenna, C., Davy, P., Brun, J.P., Funiciello, R., Mattei, M. & Nalpas, T., 1996. The opening of the Tyrrhenian sea: an experimental approach, *Geophys. J. Int.,* **126,** 781–795.

Frepoli, A. & Amato, A., 1997. Contemporaneous extension and compression in the Northern Apennines from earthquakes fault-plane solutions, *Geophys. J. Int.,* **129,** 368–388.

Gardi, A., Cocco, M., Negredo, A.M., Sabadini, R. & Singh, S.K., 2000. Dynamic modelling of the subduction zone of central Mexico, *Geophys. J. Int.,* **143,** 809–820.

Giunchi, C., Gasperini, P., Sabadini, R. & D'Agostino, G., 1994. The role of subduction on the horizontal motions in the Tyrrhenian Basin: a numerical model, *Geophys. J. Int.,* **21,** 529–532.

Giunchi, C., Kiratzi, A., Sabadini, R. & Louvari, E., 1996a. A numerical model of the Hellenic subduction zone: active stress field and sea-level changes, *Geophys. Res. Lett.,* **23,** 2485–2488.

Giunchi, C., Sabadini, R., Boschi, E. & Gasperini, P., 1996b. Dynamic models of subduction: geophysical and geological evidence in the Thyrrenian Sea, *J. Int. Geophys. Res. Papers,* **126,** 555–578.

Goodman, R.E., Taylor, R.L. & Brekke, T.L., 1968. A model for the mechanics of jointed rock, *J. Soil Mech. Found. Div. Am. Soc. Civ. Eng.,* **94,** 637–658.

Hirth, G. & Kohlstedt, D.L., 1996. Water in the oceanic upper mantle: implications for rheology, melt extraction and the evolution of the lithosphere, *Earth planet. Sci. Lett.,* **144,** 93–108.

Houseman, G. & Gubbins, D., 1997. Deformation and subducted oceanic lithosphere, *Geophys. J. Int.,* **131,** 535–551.

Huismans, R.S., Podladchikov, Y.Y. & Cloetingh, S., 2001. Transition from passive to active rifting: relative importance of asthenospheric doming and passive extension of the lithosphere, *J. geophys. Res.,* **106,** 11 271–11 291.

Hunstad, I., Anzidei, M., Cocco, M., Baldi, P., Galvani, A. & Pesci, A., 1998. Modelling coseismic displacement during the 1997 Umbria–Marche earthquake (Central Italy), *Geophys. J. Int.,* **139,** 283–295.

Irifune, T. & Ringwood, A.E., 1987. Phase transformations in a harzburgite composition to 26 GPa: implications for dynamic behaviour of the subducting slab, *Earth planet. Sci. Lett.,* **86,** 365–376.

Jimenez Munt, I., Sabadini, R., Gardi, A. & Bianco, G., 2003. Active deformation in the mediterranean from Gibraltar to Anatolia inferred from numerical modelling, geodetic and seismological data, *J. geophys. Res.,* **108**(B1), 2006, doi:10.1029/2001JB001544.

Lavecchia, G., 1988. The Tyrrhenian–Apennines system: structural setting and seismotectonogenesis, *Tectonophysiscs,* **147,** 263–296.

Malinverno, A. & Ryan, W.B.F., 1986. Extension in the Tyrrhenian Sea and shortening in the Apennines as result of arc migration driven by sinking of the lithosphere, *Tectonics,* **5,** 227–245.

Meghraoui, M., Bosi, V. & Camelbeeck, T., 1999. Fault fragment control in Umbria–Marche, Central Italy, earthquake sequence, *Geophys. Res. Lett.,* **26,** 1069–1072.

Mele, G., Rovelli, A., Seber, D. & Barazangi, M., 1997. Shear wave attenuation in the lithosphere beneath Italy and surrounding regions: tectonic implications, *J. geophys. Res.,* **102,** 11 863–11 875.

Mongelli, F., Zito, G., Della Vedova, B., Pellis, G., Squarci, P. & Taffi, L., 1991. Geothermal regime of Italy and surrounding seas, in *Exploration of the Deep Continental Crust,* eds Cermak, V. & Rybach, L., Springer-Verlag, Berlin.

Montone, P., Amato, A. & Pondrelli, S., 1999. Active stress map of Italy, *J. geophys. Res.,* **104,** 25 595–25 610.

MSC.Marc, 2001. *Volume A: Theory and User Information,* MSC.Software Corporation (www.marc.com).

Mueller, B., Reinecker, J. & Fuchs, K., 2000. The 2000 release of the World Stress Map (www.world-stress-map.org).

Negredo, A.M., Carminati, E., Barba, S. & Sabadini, R., 1999a. Dynamic modelling of stress accumulation in Central Italy, *Geophys. Res. Lett.,* **26,** 1945–1948.

Negredo, A.M., Sabadini, R., Bianco, G. & Fernandez, M., 1999b. Three-dimensional modelling of crustal motions caused by subduction and continental convergence in the central Mediterranean, *Geophys. J. Int.,* **136,** 261–274.

Patacca, E., Sartori, R. & Scandone, P., 1990. Tyrrhenian Basin and Apenninic arcs: kinematic relations since later Tortonian times, *Mem. Soc. Geol. It.,* **45,** 425–451.

Pialli, G., Barchi, M. & Minelli, G., eds, 1998. Results of the CROP-03 deep seismic reflection profile, *Mem. Soc. Geol. It.,* **52**.

Piromallo, C. & Morelli, A., 1997. Imaging the Mediterranean upper mantle by *P*-wave travel time tomography, *Ann. Geofis.,* **XL,** 963–979.

Pollitz, F.F., Peltzer, G. & Burgmann, R., 2000. Mobility of continental mantle: evidence from postseismic geodetic observations following the 1992 Landers earthquake, *J. geophys. Res.,* **105,** 8035–8054.

Rebaï, S., Philip, H. & Taboada, A., 1992. Modern tectonic stress field in the Mediterranean region: evidence for variation in stress directions at different scales, *Geophys. J. Int.,* **110,** 106–140.

Rehault, J.P., Boillot, G. & Mauffret, A., 1984. The western Mediterranean Basin geological evolution, *Mar. Geol.,* **55,** 447–492.

Ricci Lucchi, F., 1986. The Oligocene to recent foreland basins of the Northern Apennines, *Spec. Publ. Int. Assoc. Sediment.,* **8,** 105–139.

Riva, R., Aoudia, A., Vermeersen, L.L.A., Sabadini, R. & Panza, G.F., 2000. Crustal versus asthenospheric relaxation and post-seismic deformation for shallow normal faulting earthquakes: the Umbria–Marche (central Italy) case, *Geophys. J. Int.,* **141,** F7–F11.

Sartori, R., 1989. Evoluzione neogenico recente del bacino tirrenico e suoi rapporti con la geologia delle aree circostanti, *G. Geol.,* **51,** 1–39.

Selvaggi, G. & Amato, A., 1992. Subcrustal earthquakes in northern Apennines (Italy): evidence for a still active subduction?, *Geophys. Res. Lett.,* **19,** 2127–2130.

Serri, G., Innocenti, F. & Manetti, P., 1993. Geochemical and petrological evidence of the subduction of delaminated Adriatic continental lithosphere in the genesis of the Neogene–Quaternary magmatism of central Italy, *Tectonophysics,* **223,** 117–147.

Spada, G., Ricard, Y. & Sabadini, R., 1992. Excitation of true polar wander by subduction, *Nature,* **360,** 452–454.

Spadini, G., Cloetingh, S.A.P.L. & Bertotti, G., 1995. Thermo-mechanical modeling of the Tyrrhenian Sea: lithosphere necking and kinematics of rifting, *Tectonics,* **14,** 629–644.

Spakman, W., 1990. Tomographic images of the upper mantle below central Europe and the Mediterranean, *TerraNova,* **2,** 542–553.

Turcotte, D.L. & Shubert, G., 2001. *Geodynamics,* p. 269, Wiley, New York.

Valensise, G. & Pantosti, D., 2001. Database of potential sources for earthquakes larger than *M* 5.5 in Italy. Version 2.0, *Ann. Geofis.,* **44,** 4, 797–964.

Wezel, F.C., 1982. The Tyrrhenian sea: a rifted krikogenic swell basin, *Mem. Soc. Geol. It.,* **24,** 531–568.

Whittaker, A., Bott, M.H.P. & Waghorn, G.D., 1992. Stresses and plate boundary forces associated with subduction plate margins, *J. geophys. Res.,* **97,** 11 933–11 944.

Wortel, M.J.R. & Spakman, W., 2000. Subduction and slab detachment in the Mediterranean–Carpathian region, *Science,* **290,** 1910–1917.